

Study of manganese germanides formation and their magnetic response

Omar Abbes^{1,*}, Alain Portavoce², Christophe Girardeaux², Lisa Michez³, Vinh Le Thanh³

¹GREMI CNRS-Université d'Orléans, 14 Rue d'Issoudun, Orléans, 45067, France

²Aix-Marseille Université, CNRS, IM2NP-UMR 6242, Saint Jérôme Case 142, Marseille, 13397, France

³Aix-Marseille Université, CNRS, CINaM-UMR 7325, Luminy Case 913, Marseille, 13288, France

*Corresponding author, Tel: (+33) 238417123; E-mail: omar.abbes@univ-orleans.fr

Received: 10 May 2016, Revised: 16 September 2016 and Accepted: 02 October 2016

DOI: 10.5185/amlett.2017.6908

www.vbripress.com/aml

Abstract

The Mn-Ge binary system is a potential candidate to the fabrication of Spintronic devices. However, the understanding of the contribution of each possible Mn-Ge phase is crucial. In this work, the reaction between 50 nm thick Mn film and amorphous Ge substrate was studied via *in-situ* XRD. These experiments lead to the identification of the Mn-germanides formed during the reaction, with structural and magnetic confirmation. Besides, a sequence of germanides formation is studied and proposed. Copyright © 2017 VBRI Press.

Keywords: Manganese, germanium, spintronics, reactive diffusion.

Introduction

For so many years, coupling magnetic and semiconducting properties in the same material has attracted an interest of developing spintronic field activities. Two major ways are used to provide this coupling. The first one is using Diluted Magnetic Semiconductors (DMS) as a spin aligner [1-4], the second one is to use ferromagnetic metal/semiconductor heterostructures via a Schottky barrier [5] or an insulator [6]. Using a Si- or Ge-based DMS would be perfect since they have a natural impedance match with Si or Ge, the two semiconductors in the existing Si Complementary Metal Oxide Semiconductor (CMOS) technology. But most of those DMSs present generally a Curie Temperature (T_C) lower than 200 K, and a low concentration of magnetic elements because of their low solubility in the semiconductor matrix [7]. Hence, the formation of precipitates could eventually limit their incorporation in a spin injection device.

Concerning the second method, interesting results were shown for the Fe/GaAs system [8], but for spin injection into group-IV semiconductors (Ge and Si), the efficiency is still very small. Most of the silicides or germanides formed by reaction of a ferromagnetic metal (Fe, Co, Ni...) with Si or Ge are not ferromagnetic. Besides, the growth of an epitaxial oxide grown between Ge or Si and a ferromagnetic metal is not easy [9]. However, the Mn_5Ge_3 compound has been attracting a lot of interest in recent years [10-13]. For example, theoretical calculations assumed high spin-injection efficiency for this compound [14], with a demonstrated spin polarization up to 42% [15]. In addition, Mn_5Ge_3 thin films can be

epitaxially grown on Ge(111) substrates [16,17], that would allow a direct spin injection of into Ge. Therefore, Mn_5Ge_3 with its relatively high T_C either for bulk or for thin films [18, 19] is a potential candidate for injecting a spin-polarized current into semiconductors (Ge, Si) without an external applied magnetic field, by tunnel effect through the Schottky barrier.

The elaboration of this germanide throughout reaction between a metal and Ge, is an example of reactive diffusion (like reactions used to establish metallic contacts in integrated circuits technology [20]). However, it is not the only one present in the Ge-Mn bulk phase diagram, there are four phases at standard pressure and temperature conditions: $Mn_{3,4}Ge$, Mn_7Ge_3 , Mn_5Ge_3 and $Mn_{11}Ge_8$ [21]. In this paper, we investigate the phase formation of the Mn-germanides by reaction between a submicrometric Mn film and a Ge amorphous substrate. X-Ray Diffraction (XRD), Superconducting QUantum Interference Device (SQUID) magnetometer and Transmission Electron Microscopy (TEM) were used to study the Mn-Ge reaction, to identify the phases formed during annealing and to characterize them.

Experimental

A 120 nm thick SiO_2 oxide grown on Si(100) was used as substrate, which served as a support for amorphous Ge deposition. The substrates were cleaned chemically with an ultrasonic rinsing in ethanol and acetone, in order to eliminate hydrocarbon contaminants, prior to their introduction into the deposition chamber. This chamber exhibits a base pressure better than 5.10^{-9} mbar equipped with an evaporator set-up and high purity Mn and Ge

charges (~ 99.999 wt.%). By the mean of electron beam evaporation, a 150 nm thick film of amorphous Ge film (a-Ge) was first deposited, than 50 nm thick Mn layer topped the sample. Both depositions were executed at room temperature, with a rate of 0.2 nm/s. X-Ray Reflectivity permitted to determine the thicknesses of the Mn and Ge layers. In Fig. 1 is shown the X-Ray spectrum between 0.9° and 1.8° with one spectrum executing two modulations, the bigger modulation corresponds to the thinner film, while the small modulation corresponds to the thicker layer.

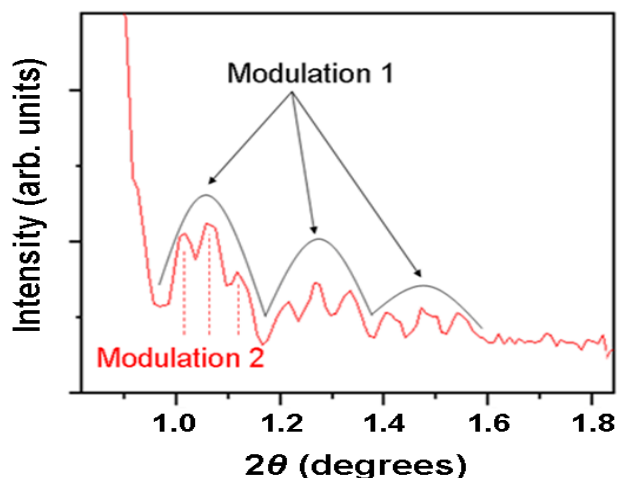


Fig. 1. X-Ray Reflectivity spectrum for 2θ between 0.9° and 1.8° showing two modulations corresponding to the thicknesses of Mn and Ge layers deposited on substrates.

The found thicknesses were 48.7 nm for Mn, and 153.6 nm for Ge. They were obtained using the simplified Bragg's law ($e \cdot \Delta(2\theta) = \lambda$ with e the thickness of the film, $\Delta(2\theta)$ the angular difference between the same modulation peaks and λ the wave length of the used rays). Reaction between Mn and Ge was monitored by XRD in the Bragg–Brentano geometry in a vacuum chamber with a pressure of $5 \cdot 10^{-5}$ mbar, and Cu $K\alpha$ source with $\lambda_{K\alpha} = 0.154$ nm. During XRD measurements, the temperature was increased by steps using a ramp of $5^\circ\text{C}/\text{min}$. The magnetic properties of the films were probed using SQUID magnetometer with a magnetic field of 0.5 T applied in plane of the sample surface, measurements were performed between 5 K and 350 K. Structural characterization of grown phases was performed by means of High Resolution Transmission Electron Microscopy (HR-TEM) using a JEOL 3010 microscope operating at 300 kV with a spatial resolution of 1.7 Å.

Results and discussions

This section will be divided into two subsections in which we present results concerning the growth of Mn-germanides as well as their magnetic and structural properties.

Phases grown during Mn-Ge reaction

In order to determine the phase formation sequence during Mn-Ge solid state reaction, *in-situ* XRD

measurements were carried up upon two samples. Both samples were annealed under the same conditions in the XRD chamber. At room temperature, just one peak of Mn(330) can be detected in the 2θ (diffraction angle) window; from 20° to 60° . The peak of Mn starts to disappear as three other peaks appear at $T \sim 210^\circ\text{C}$. These peaks at $2\theta = 38.2^\circ$, 42.3° and 43.6° may respectively, correspond to the orientations: (210), (211) and (112) of Mn_5Ge_3 [22].

Using a ramp of $5^\circ\text{C}/\text{min}$, and a spectrum recorded each 5°C , no other peaks were detected. The intensity of the three peaks reaches its maximum at $T \sim 300^\circ\text{C}$, after the entire consumption of Mn. In Fig. 2 is shown the XRD spectrum corresponding to the sample annealed at 300°C , as well as the one corresponding to the second sample annealed at 650°C . While we carried out the annealing of the second sample, we noticed that Mn_5Ge_3 peaks' intensity decreased, and six other peaks appear at $T \sim 310^\circ\text{C}$. Those six peaks are detected at $2\theta = 27.2^\circ$, 34.6° , 40.3° , 45.3° , 53.6° and 58.4° . They can be attributed to the lattice plane families: (311), (106), (107), (421), (704) and (327) of $\text{Mn}_{11}\text{Ge}_8$. Only three of them can be assessed to the crystallized Ge families: (111), (220), and (311) at respectively $2\theta = 27.2^\circ$, 45.3° and 53.6° . The six peaks are present until the end of the annealing at 650°C , as shown in Fig. 2.

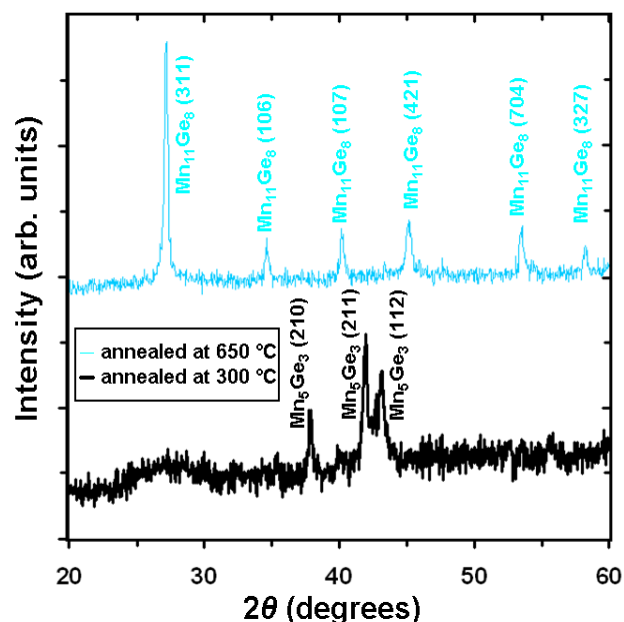


Fig. 2. XRD spectra with 2θ varying from 20° to 60° , of two samples annealed with a ramp of $5^\circ\text{C}/\text{min}$, from room temperature to 300°C for black line, and to 650°C for bright blue line.

According to the *in-situ* XRD measurements, the formation of Mn-germanides occurs sequentially; $\text{Mn} + \text{Ge} \rightarrow \text{Mn} + \text{Mn}_5\text{Ge}_3 + \text{Ge} \rightarrow \text{Mn}_5\text{Ge}_3 + \text{Ge} \rightarrow \text{Mn}_5\text{Ge}_3 + \text{Mn}_{11}\text{Ge}_8 + \text{Ge} \rightarrow \text{Mn}_{11}\text{Ge}_8 + \text{Ge}$. This scheme can be simplified as shown in Fig. 3.

During the 50 nm thick Mn film reaction with amorphous Ge, we noticed that Mn_5Ge_3 is the first phase to be formed under conditions used ($5^\circ\text{C}/\text{min}$ temperature ramp). The scenario that we propose to the Mn-Ge phase

formation is the following (**Fig. 3**): (i) before annealing, the Mn film is stable on the Ge substrate, (ii) after annealing, Mn is consumed in reaction with Ge in order to form Mn_5Ge_3 at the interface Mn/Ge, then (iii), Mn_5Ge_3 grow until the whole consumption of Mn, at this step only Mn_5Ge_3 and Ge are present. Carrying out the annealing (iv) a second phase richer in Ge, $\text{Mn}_{11}\text{Ge}_8$, is formed by consuming partially Mn_5Ge_3 and Ge, eventually at the interface $\text{Mn}_5\text{Ge}_3/\text{Ge}$. Finally, (v) Mn_5Ge_3 is totally consumed and the only phase present is $\text{Mn}_{11}\text{Ge}_8$ at the top of the Ge substrate.

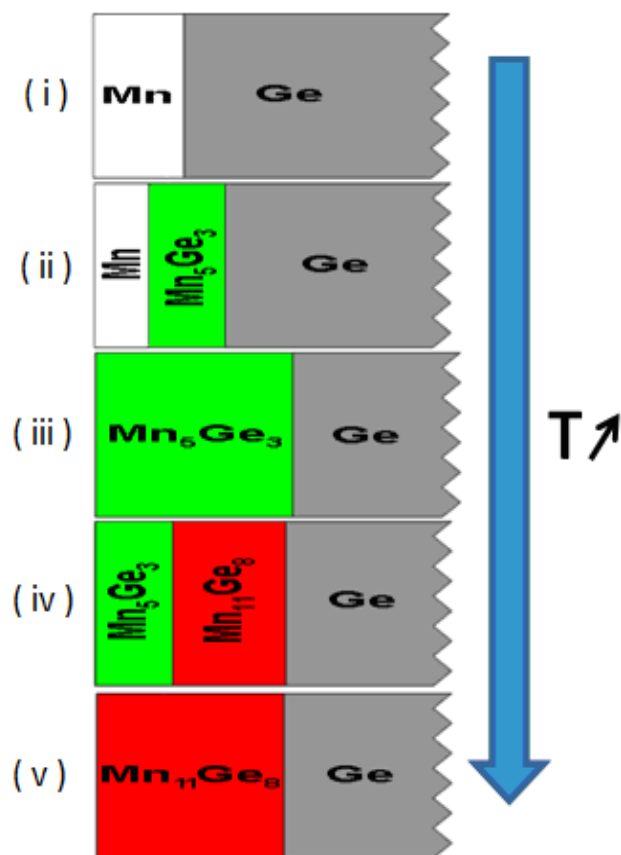


Fig. 3. Reaction scenario of a 50 nm thick Mn film deposited on 150 nm a-Ge substrate.

Structural and magnetic properties of the phases

Two samples, containing each one just one phase, were prepared for microscopic and magnetic ex-situ characterizations: the first one is annealed at 300 °C (with only XRD peaks of Mn_5Ge_3), and the second one is annealed at 650 °C (with XRD peaks of $\text{Mn}_{11}\text{Ge}_8$).

TEM image of the structure of the sample (annealed at 300 °C) is presented in **Fig. 4(a)**. This image displays atomic planes thanks to the grains' orientations in the polycrystalline Mn_5Ge_3 layer. In this region, atomic rows are distinguishable, they are separated by 2.3 Å which corresponds to the interatomic distance of $\text{Mn}_5\text{Ge}_3(210)$ planes. The XRD peak of these planes can be easily seen in **Fig. 2**.

For the sample annealed at 650 °C, with just $\text{Mn}_{11}\text{Ge}_8$ layer that corresponds likely to the only phase detected by XRD, TEM image is presented in **Fig. 4(b)**. By

examining the distance between atomic planes of this layer, we found that there are interplanar distances corresponding to this phase. Experimental measurements of the interplanar distance give about 4.5 Å, which corresponds exactly to the distance of the planes' family $\text{Mn}_{11}\text{Ge}_8(111)$. The corresponding XRD peak is located at $2\theta \approx 19^\circ$, therefore we could not detect it at the XRD 2θ window used: (20°-60°).

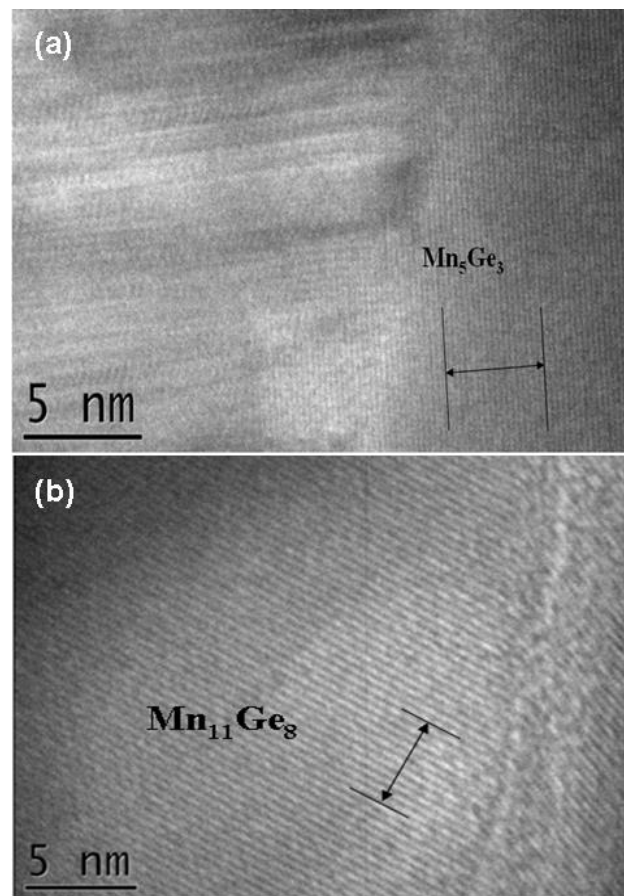


Fig. 4. High resolution TEM cross section images taken over (a) the sample annealed at 300 °C, and (b) the sample annealed at 650 °C.

The magnetic characterizations by SQUID, are presented in **Fig. 5**. Hence, the temperature dependence of the magnetization of the two prepared samples (annealed at 300 °C and 650 °C) is presented. For the sample annealed at 300 °C (presented by purple diamonds curve in **Fig. 5**), as the temperature increases, the magnetization decreases slightly between 5 K and 250 K, then decreases gradually to reach almost zero after 300 K. This attitude is typically characteristic of a ferromagnetic material, with a ferromagnetic - paramagnetic transition at the Curie temperature. The measured T_C is 297 K, it coincides with the inflection point of the slope of the magnetization. It is the same temperature as for bulk Mn_5Ge_3 material [18].

The magnetization of the sample annealed at 650 °C is presented by blue squares curve in **Fig. 5**. It decreases rapidly between 5 K and 100 K, and then it increases slightly to reach a maximum around 140 K. And finally, beyond 150 K, magnetization decreases again until reaching an almost equal zero value at $T \sim 300$ K. Two

transitions are hence distinguished. The first one corresponds to ferromagnetic - paramagnetic transition at Curie temperature $T_C = 45$ K, while the second one corresponds to antiferromagnetic - ferromagnetic transition at a temperature called Neel temperature: $T_N = 140$ K.

$Mn_{11}Ge_8$ exhibits antiferromagnetic - ferromagnetic transition at $T \sim 150$ K, as confirmed by XRD and TEM measurements, it is the phase that has got the biggest volume in the sample annealed at 650 °C. This magnetic signature is similar to the one obtained by Cho *et al.* [23], and that corresponds to $Mn_{11}Ge_8$. One can therefore, link this signature to $Mn_{11}Ge_8$.

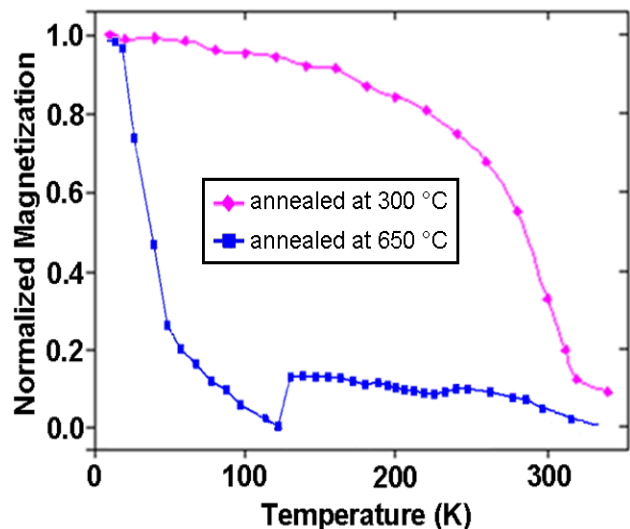


Fig. 5. Evolution of the normalized magnetization versus temperature (between 5 K and 350 K) of the sample annealed up to 300 °C (blue square), and the sample annealed up to 650 °C (purple diamond), with a magnetic field applied in-plane of sample.

The Curie temperature measured at 45 K does not correspond to a known phase of the Mn-Ge diagram at low temperature conditions (< 650 °C). The measured magnetization versus temperature could be the result of the convolution of multiple magnetization curves, which means that multiple phases can exist in the sample. The measured Curie temperature at 45 K was attributed in a recent study to ferromagnetic nano-clusters formed by Mn, Ge and C atoms [24].

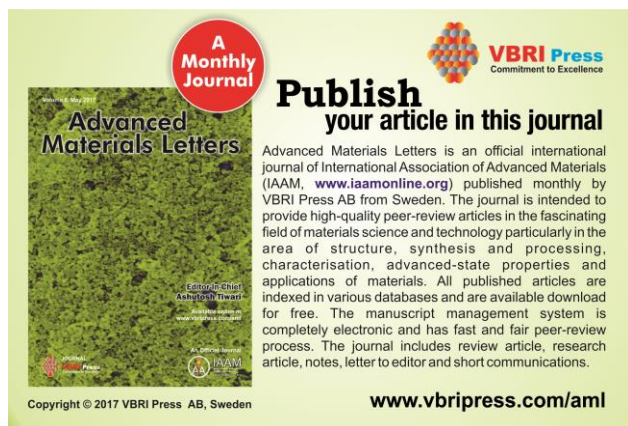
Conclusion

In conclusion, Mn-Ge solid state reaction was investigated by *in-situ* XRD. The result of the reaction between 50 nm-thick Mn layer and amorphous Ge substrate is a sequential phase formation. Two phases appear in the sequence: Mn_5Ge_3 the first phase to grow, and $Mn_{11}Ge_8$ that appears only after the whole Mn layer consumption. Mn_5Ge_3 being the ferromagnetic compound, could be stabilized for spintronic applications. Structural and magnetic characterizations of the phases confirmed the results obtained by XRD. However, in addition to the antiferromagnetic $Mn_{11}Ge_8$ phase, SQUID measurements revealed the presence of ferromagnetic structure in the sample annealed at 650 °C.

References

- Cho, S.; Choi, S.; Hong, S.C.; Kim, Y.; Ketterson, J.B.; Kim, B.-J.; Kim, Y.C.; Jung, J.-H.; *Phys. Rev. B*, **2002**, *66*, 033303. DOI: [10.1103/PhysRevB.66.033303](https://doi.org/10.1103/PhysRevB.66.033303)
- Ayoub, J.-P.; Favre, L.; Berbezier, I.; Ronda, A.; Morresi, L.; Pinto, N.; *Appl. Phys. Lett.*, **2007**, *91*, 141920. DOI: [10.1063/1.2794723](https://doi.org/10.1063/1.2794723)
- Zeng, C.; Zhang, Z.; van Benthem, K.; Chisholm, M.F.; Weitering, H.H.; *Phys. Rev. Lett.*, **2008**, *100*, 066101. DOI: [10.1103/PhysRevLett.100.066101](https://doi.org/10.1103/PhysRevLett.100.066101)
- Dolph, M.C.; Kim, T.; Yin, W.; Recht, D.; Fan, W.; Yu, J.; Aziz, M.J.; Lu, J.; Wolf, S.A.; *J. Appl. Phys.*, **2011**, *109*, 093917. DOI: [10.1063/1.3590137](https://doi.org/10.1063/1.3590137)
- Hanbicki, A.T.; Jonker, B.T.; Itskos, G.; Kioseoglou, G.; Petrou, A.; *Appl. Phys. Lett.*, **2002**, *80*, 1240. DOI: [10.1063/1.1449530](https://doi.org/10.1063/1.1449530)
- Jiang, X.; Wang, R.; Shelby, R.M.; Macfarlane, R.M.; Bank, S.R.; Harris, J.S.; Parkin, S.S.P.; *Phys. Rev. Lett.*, **2005**, *94*, 056601. DOI: [10.1103/PhysRevLett.94.056601](https://doi.org/10.1103/PhysRevLett.94.056601)
- Woodbury, H.H.; Tyler, W.W.; *Phys. Rev.*, **1955**, *100*, 659. DOI: [10.1103/PhysRev.100.659](https://doi.org/10.1103/PhysRev.100.659)
- Li, C.H.; Kioseoglou, G.; van't Erve, O.M.J.; Hanbicki, A.T.; Jonker, B.T.; Mallory, R.; Yasar, M.; Petrou, A.; *Appl. Phys. Lett.*, **2004**, *85*, 1544-1546. DOI: [10.1063/1.1786366](https://doi.org/10.1063/1.1786366)
- Jonker, B.T.; Kioseoglou, G.; Hanbicki, A.T.; Li, C.H.; Thompson, P.E.; *Nat. Phys.*, **2007**, *3*, 542. DOI: [10.1038/nphys673](https://doi.org/10.1038/nphys673)
- Zeng, C.; Erwin, S.C.; Feldman, L.C.; Li, A.P.; Jin, R.; Song, Y.; Thompson, J.R.; Weitering, H.H.; *Appl. Phys. Lett.*, **2003**, *83*, 5002. DOI: [10.1063/1.1633684](https://doi.org/10.1063/1.1633684)
- Olive-Mendez, S.; Spiesser, A.; Michez, L.A.; Le Thanh, V.; Glachant, A.; Derrien, J.; Devillers, T.; Barski, A.; Jamet, M.; *Thin Solid Films*, **2008**, *517*, 191. DOI: [10.1016/0925-8388\(93\)90888-T](https://doi.org/10.1016/0925-8388(93)90888-T)
- Abbes, O.; Portavoce, A.; Le Thanh, V.; Girardeaux, C.; Michez, L.; *Appl. Phys. Lett.*, **2013**, *103*, 172405. DOI: [10.1063/1.4827100](https://doi.org/10.1063/1.4827100)
- Abbes, O.; Xu, F.; Portavoce, A.; Girardeaux, C.; Hoummada, K.; Le Thanh, V.; *Defect Diffus. Forum*, **2012**, *323-325*, 439. DOI: [10.4028/www.scientific.net/DDF.323-325.439](https://doi.org/10.4028/www.scientific.net/DDF.323-325.439)
- Picozzi, S.; Continenza, A.; Freeman, A.J.; *Phys. Rev. B*, **2004**, *70*, 235205. DOI: [10.1103/PhysRevB.70.235205](https://doi.org/10.1103/PhysRevB.70.235205)
- Panguluri, R.P.; Zeng, C.; Weitering, H.H.; Sullivan, J.M.; Erwin, S.C.; Nadgorny, B.; *Phys. Status Solidi B*, **2005**, *242*, R67. DOI: [10.1002/pssb.200510030](https://doi.org/10.1002/pssb.200510030)
- Spiesser, A.; Olive-Mendez, S.F.; Dau, M.-T.; Michez, L.A.; Watanabe, A.; Le Thanh, V.; Glachant, A.; Derrien, J.; Barski, A.; Jamet, M.; *Thin Solid Films*, **2010**, *518*, S113. DOI: [10.1016/j.tsf.2009.10.067](https://doi.org/10.1016/j.tsf.2009.10.067)
- Choi, S.; Hong, S.C.; Cho, S.; Kim, Y.; Ketterson, J.B.; Jung, C.-U.; Rhie, K.; Kim, B.-J.; Kim, Y.C.; *J. Appl. Phys.*, **2003**, *93*, 7670. DOI: [10.1063/1.1558611](https://doi.org/10.1063/1.1558611)
- Hirai, C.; Sato, H.; Kimura, A.; Yaji, K.; Iori, K.; Taniguchi, M.; Hiraoka, K.; Muro, T.; Tanaka, A.; *Physica B: Condensed Matter*, **2004**, *351*, 341. DOI: [10.1016/j.physb.2004.06.048](https://doi.org/10.1016/j.physb.2004.06.048)
- Sawatzky, E.; *J. Appl. Phys.*, **1971**, *42*, 1706. DOI: [10.1063/1.1660402](https://doi.org/10.1063/1.1660402)
- Abbes, O.; Melhem, A.; Boulmer-Leborgne, C.; Semmar, N.; *Adv. Mater. Lett.*, **2015**, *6*, 961-964. DOI: [10.5185/amlett.2015.6138](https://doi.org/10.5185/amlett.2015.6138)
- Gokhale, A.; Abbaschian, G.J.; *Binary Alloy Phase Diagrams ASM International 2nd ed.*, **1990**, *2*, 1964. DOI: [10.1007/BF02898261](https://doi.org/10.1007/BF02898261)
- JCPDS (International Center for Diffraction Data®, Newtown Square, PA, **1997-2016**). <http://www.icdd.com/>

23. Cho, Y.M.; Yu, S.S.; Ihm, Y.E.; Kim, D.; Kim, H.; Baek, J.S.; Kim, C.S.; Lee, B.T.; *Journal of Magnetism and Magnetic Materials*, **2004**, 282, 385.
DOI: [10.1016/j.jmmm.2004.04.089](https://doi.org/10.1016/j.jmmm.2004.04.089)
24. Portavoce, A.; Abbas, O.; Spiesser, A.; Girardeaux, C.; Michez, L.; Le Thanh, V.; *Scripta Materialia*, **2015**, 100, 70.
DOI: [10.1016/j.scriptamat.2014.12.016](https://doi.org/10.1016/j.scriptamat.2014.12.016)



A Monthly Journal

Publish your article in this journal

Advanced Materials Letters is an official international journal of International Association of Advanced Materials (IAAM, www.iaamonline.org) published monthly by VBRI Press AB from Sweden. The journal is intended to provide high-quality peer-review articles in the fascinating field of materials science and technology particularly in the area of structure, synthesis and processing, characterisation, advanced-state properties and applications of materials. All published articles are indexed in various databases and are available download for free. The manuscript management system is completely electronic and has fast and fair peer-review process. The journal includes review article, research article, notes, letter to editor and short communications.

www.vbripress.com/aml

Copyright © 2017 VBRI Press AB, Sweden